Available online at www.sciencedirect.com
ScienceDirect
Ceramics International 38 (2012) 707–711
CERAMICS INTERNATIONAL
www.elsevier.com/locate/ceramint

Effect of BNBTKNN on the electrical properties of bismuth ferrite thin films

Yuanyu Wang

College of Materials Science and Metallurgy Engineering, Guizhou University, Guiyang 550003, PR China

Received 19 July 2011; received in revised form 26 July 2011; accepted 26 July 2011
Available online 3rd August 2011

Abstract

$BiFeO_3$/[0.93($Bi_{0.50}Na_{0.50}TiO_3$)–0.05$BaTiO_3$–0.02$K_{0.50}Na_{0.50}NbO_3$] (BFO/BNBTKNN) bilayered thin films were fabricated on Pt/TiO_2/SiO_2/Si substrates without any buffer layers by a combined sol–gel and radio frequency sputtering route. Effect of BNBTKNN on electrical properties of BFO/BNBTKNN thin films was investigated. A higher phase purity and a denser microstructure are induced for the BFO/BNBTKNN bilayered thin film by using the bottom BNBTKNN layer, resulting in its lower leakage current density. Moreover, the enhancement in dielectric behavior is also demonstrated for such a bilayer, where a high dielectric constant and a low dielectric loss are obtained. The BFO/BNBTKNN bilayered thin film has an improved multiferroic behavior: $2P_r \sim 76.8$ μC/cm^2, $2E_c \sim 378.1$ kV/cm, $2M_s \sim 52.6$ emu/cm^3, and $2H_c \sim 453.6$ Oe, together with a low fatigue rate up to $\sim 1 \times 10^9$ switching cycles.

Keywords: $BiFeO_3$; BNBTKNN; Multiferroic behavior; Fatigue behavior

1. Introduction

Much attention has been recently given to the multiferroic bismuth ferrite ($BiFeO_3$, BFO) material, owing to its excellent electrical properties, a high Curie temperature, and environmental friendliness [1–8]. BFO thin films with good electrical properties are considered as a promising candidate material for the high-density ferroelectric random access memories, spintronics, sensors and actuators [1,2]. However, its high leakage current density at room temperature seriously hinders the abovementioned practical application [9].

Some measurements have been used to improve ferroelectric properties of BFO thin films by reducing the leakage current density, such as a single crystal substrate [1,2,8], a oxide buffer layer [1,2,8,10,11], a multilayer structure [12–17], and an ion substitution [18–22]. Among these attempts, the multilayer structure is a promising way to improve electrical properties of ferroelectric materials [12–17]. Improved ferroelectric properties have been induced by constructing the multilayer thin films consisting of BFO and other ferroelectric layers, where these ferroelectric layers (i.e., PbZr, TiO_3 and $Bi_{0.50}Na_{0.50}TiO_3$) possess a high resistance [12–17]. 0.93($Bi_{0.5}Na_{0.5}TiO_3$)–0.05$BaTiO_3$–0.02$K_{0.5}Na_{0.5}NbO_3$ (BNBTKNN) is of a famous lead-free ferroelectric, and has good ferroelectric properties and giant strain [23]. However, there are no reports on the preparation and electrical properties of the multilayered thin film consisting of BFO and BNBTKNN layers. Therefore, it is of great interest to investigate the microstructure and electrical properties of BFO/BNBTKNN multilayered thin films.

In the present work, the BFO thin film has been fabricated by using the BNBTKNN as a buffer layer for reducing its leakage current density, where the BFO/BNBTKNN bilayered thin film has been grown by using a combined route of sol–gel and radio frequency (*rf*) sputtering. An enhancement in multiferroic behavior is observed for such a bilayered thin film, and the underlying physics mechanisms are discussed.

2. Experimental procedure

Two layers of BNBTKNN and BFO were grown by the sol–gel and *rf* sputtering technique, respectively, where the BNBTKNN layer was grown between BFO layer and Pt/TiO_2/SiO_2/Si(1 0 0) substrate. The BNBTKNN layer was prepared by the sol–gel route, where the $Ba(CH_3COO)_2$, $Bi(NO_3)_3{\cdot}5H_2O$, $Nb(OC_2H_5)_5$, KCH_3COO, $C_2H_3NaO_2$, and $Ti[OCH(CH_3)_2]_4$ are used as the starting materials. The BNBTKNN sol–gel solution was spin coated on the Pt/TiO_2/SiO_2/Si substrate at 3000 rpm for 20 s, and was then dried at 300 °C for 10 min, and baked at

E-mail address: yuanyuwang0216@163.com.

0272-8842/$36.00
doi:10.1016/j.ceramint.2011.07.061

Table 1
Preparation parameters of the BFO layer in BFO/BNBTKNN bilayered thin films.

Sample	BFO
Preparation technique	*rf* sputtering
Target-substrate distance	15 cm
Substrate temperature	550 °C
Sputtering atmosphere	Ar, O_2
Atmosphere ratio	4:1
Pressure	1.0 Pa
rf power	80 W

Table 2
Preparation parameters of the BNBTKNN layer in BFO/BNBTKNN bilayered thin films.

Sample	BNBTKNN
Preparation technique	Sol–gel
Spinning rate	3000 rpm
Dried temperature	300 °C
Baked temperature	500 °C
Crystallized temperature	750 °C

500 °C for 30 min. The BNBTKNN layer with the thickness of ~130 nm was obtained by repeating the abovementioned process for two times. The as-deposited BNBTKNN thin film was finally crystallized at ~750 °C for 2 h in air, and then the BFO layer was deposited on the BNBTKNN/Pt/TiO_2/SiO_2/Si(1 0 0) substrate by *rf* sputtering at the substrate temperature of ~550 °C. The BFO layer was deposited under a *rf* power of ~80 W, and at a deposition pressure of ~1.0 Pa with Ar and O_2 at a ratio of 4:1. The BNBTKNN and BFO single layers were grown on Pt/TiO_2/SiO_2/Si(1 0 0) substrates by using the sol–gel and *rf* sputtering technique, respectively. Detailed preparation parameters are shown in Tables 1 and 2. The top electrode with the Au dots of ~0.10 mm in radius is prepared on these thin films for measuring their electrical properties.

The phase structure of thin films was measured by X-ray diffraction (XRD) (DX-100, Dandong, China). Scanning electron microscopy (SEM) (Philips, XL30) was employed to study the cross section and surface morphologies of thin films. Fatigue behavior and ferroelectric properties of thin films were conducted by the Radiant precise workstation (RT2000 Tester, USA). The magnetic behavior of thin films was carried out by the superconducting quantum interference devices (SQUID, San Diego, CA). Dielectric properties of thin films were measured by Hp4294.

3. Results and discussion

Fig. 1 shows the XRD patterns for the BFO, BNBTKNN, and BFO/BNBTKNN thin films. The BNBTKNN thin film has a pure phase with a (1 1 0) orientation, while the BFO phase cannot be formed when deposited on the Pt/TiO_2/SiO_2/Si(1 0 0) substrate without any buffer layers, where a number of secondary phases are observed. The BFO/BNBTKNN bilayered thin film has a pure phase with a polycrystalline

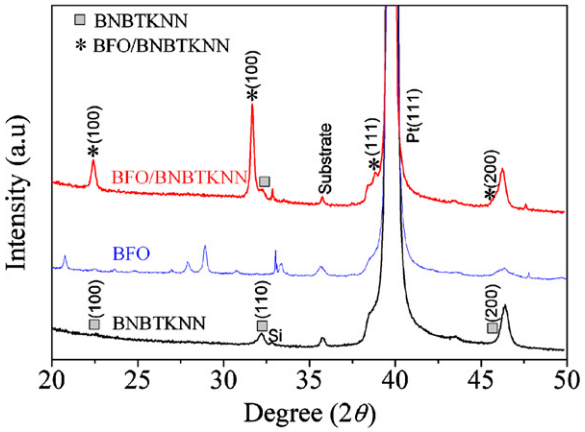

Fig. 1. XRD patterns for BFO, BNBTKNN, and BFO/BNBTKNN thin films.

structure, and the improvement in phase purity can be attributed to the induced growth of the BNBTKNN layer. Therefore, it is a good approach to improve the phase purity of bismuth ferrite thin films by inserting the BNBTKNN ferroelectric layer.

Fig. 2(a) shows the cross section of the BFO/BNBTKNN thin film. The thicknesses of BFO and BNBTKNN layers are

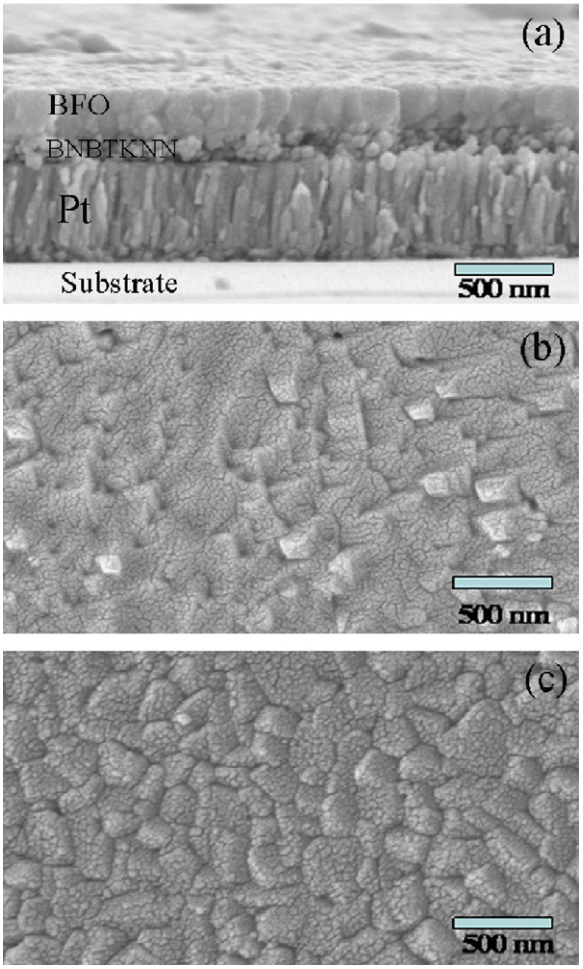

Fig. 2. (a) Cross section of the BFO/BNBTKNN bilayered thin film, and SEM surface morphologies of (b) BNBTKNN and (c) BFO/BNBTKNN thin films.

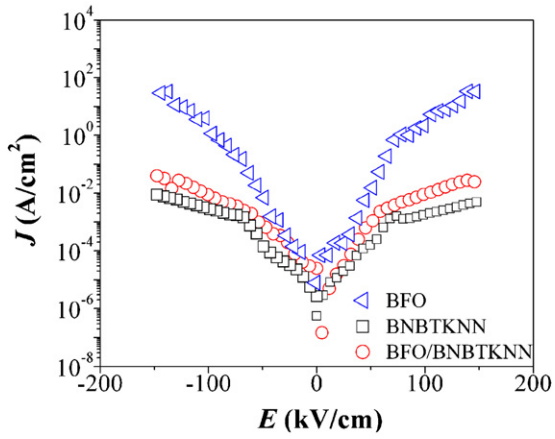

Fig. 3. J vs E curves for the BFO, BNBTKNN, and BFO/BNBTKNN thin films.

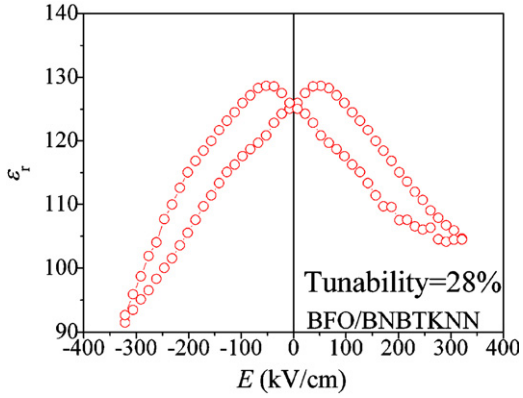

Fig. 4. C–V curve for the BFO/BNBTKNN thin film.

~280 nm and ~130 nm, respectively. The interface between thin films and Pt electrode is well established, and the BFO layer has a crack-free texture and is well adhered to the BNBTKNN layer. Fig. 2(b) and (c) shows the surface morphologies of BNBTKNN and BFO/BNBTKNN thin films, respectively. A dense microstructure is induced for the BFO/BNBTKNN bilayered thin film, owing to the introduction of the dense BNBTKNN layer. The dense microstructure should play an important role in the improvement in the ferroelectric behavior of such a bilayer.

Fig. 3 shows the leakage current J vs E for the BFO, BNBTKNN, and BFO/BNBTKNN thin films, measured at room temperature. The BNBTKNN thin film has a much lower leakage current density than that of the pure BFO thin film, which is about three orders of magnitude lower than that of the BFO thin film. As reported, the pure BFO thin film often has a very high leakage current density when deposited on the Pt-coated silicon substrate with any buffer layers [12]. A low leakage current density is induced for the BFO/BNBTKNN thin film, owing to the introduction of the BNBTKNN layer with a low leakage current density, as confirmed by the dense microstructure in Fig. 2(a) and (c).

It is important to understand the relationship between the dielectric constant of the thin film and applied electric fields. Fig. 4 shows the C–V curve of the BFO/BNBTKNN thin films measured at 100 kHz, where the dc electric field is swept from a negative bias (−330 kV/cm) to a positive bias (+330 kV/cm) and then back again. The C–V curve has a typically butterfly-type shape, and a non-linear dielectric behavior is demonstrated. The maximum in-plane dielectric tunability ($\Delta\varepsilon/\varepsilon$) can be calculated by the following formula:

$$\Delta\varepsilon = \frac{\varepsilon_{max} - \varepsilon_{min}}{\varepsilon_{max}} \quad (1)$$

where the ε_{max} and ε_{min} represent the maximum and minimum values of dielectric constant, which were measured at 0 kV/cm and the largest applied electric field. The dielectric tunability of the BFO/BNBTKNN thin film at 100 kHz is calculated to be ~28%, according to the data shown in Fig. 4.

Fig. 5(a) plots the P–E loops for the BFO/BNBTKNN thin film, measured at 5 kHz and room temperature. A remnant

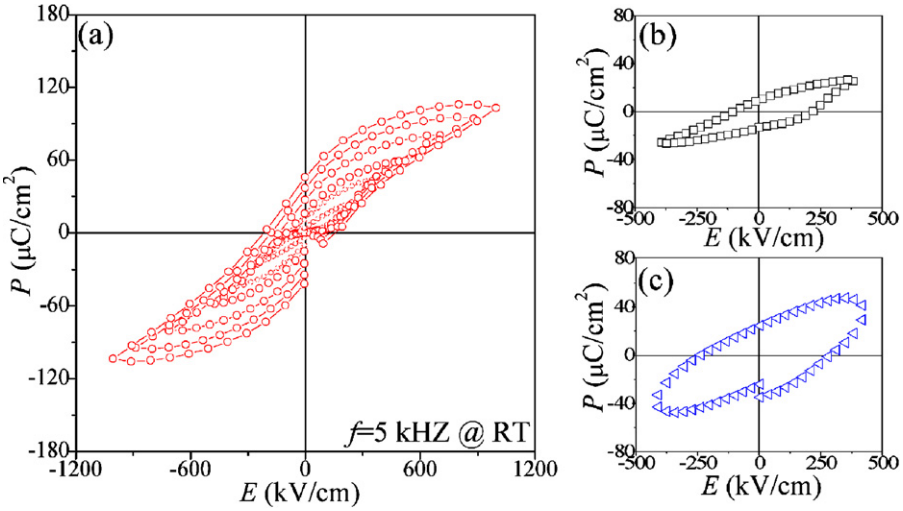

Fig. 5. P–E loops for (a) BFO/BNBTKNN, (b) BNBTKNN and (c) BFO thin films.

polarization ($2P_r$) of ~76.8 μC/cm^2 and a coercive electric field ($2E_c$) of ~378.1 kV/cm are obtained for the BFO/BNBTKNN bilayered thin film. However, a roundish *P–E* loop is observed for the BFO single-layer thin film grown on the Pt/TiO_2/SiO_2/Si(1 0 0) substrate without any buffer layers at the substrate temperature of ~550 °C, owing to the contribution of a very high leakage current density, while a better *P–E* loop is demonstrated for the BNBTKNN thin film due to its much lower leakage current density, as shown in Fig. 5(b) and (c). In the present work, the BFO/BNBTKNN bilayered thin film demonstrates improved ferroelectric properties, including a higher remnant polarization ($2P_r$) and a better hysteresis loop than those of BFO and BNBTKNN single-layer thin films. The $2P_r$ value of ~76.8 μC/cm^2 is observed for the BFO/BNBTKNN bilayered thin film, which is also more than the reported value for the BNBTKNN materials [23]. The enhancement in $2P_r$ can well be attributed to the improved phase purity crystallinity and a lower leakage current density of the BFO layer deposited on the bottom BNBTKNN layer. Moreover, the BFO/BNBTKNN bilayered thin film has a smaller E_c value than that of the BFO single layer because of the introduction of the BNBTKNN layer with a smaller E_c value [23], whereby the ferroelectric behavior is modified in the bilayer structure.

Fig. 6 plots the *M–H* loop of the BFO/BNBTKNN thin film, measured at 10 kOe and room temperature. The BFO/BNBTKNN bilayered thin film is of a typical ferromagnetic material. The saturation magnetization of the BFO layer is strongly dependent on the bottom BNBTKNN layer, although the bottom nonmagnetic BNBTKNN layer cannot contribute to the magnetic behavior of the BFO/BNBTKNN bilayered thin film. The BFO/BNBTKNN thin film shows a higher saturated magnetization ($2M_s$ ~ 52.6 emu/cm^3 and $2H_c$ ~ 453.6 Oe) than those of the pure BFO thin film reported by other authors [5,7]. The increase in M_s and H_c values can be accounted for by the interface coupling between BFO and BNBTKNN layers [12].

Fig. 7 shows the fatigue behavior of the BFO/BNBTKNN thin film as a function of switching cycles, measured at the driving electric field of ~700 kV/cm and the frequency of 100 kHz and 1 MHz. The BFO/BNBTKNN bilayered thin film

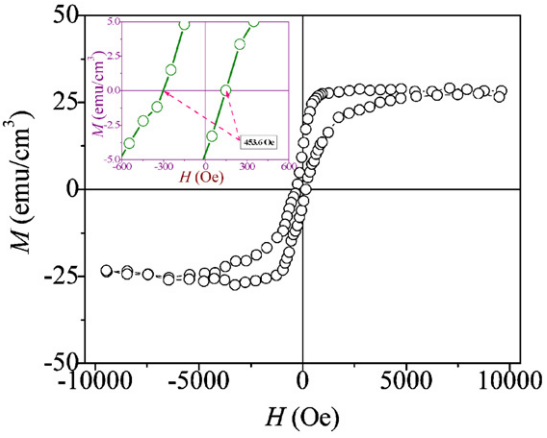

Fig. 6. *M–H* loop for the BFO/BNBTKNN thin film.

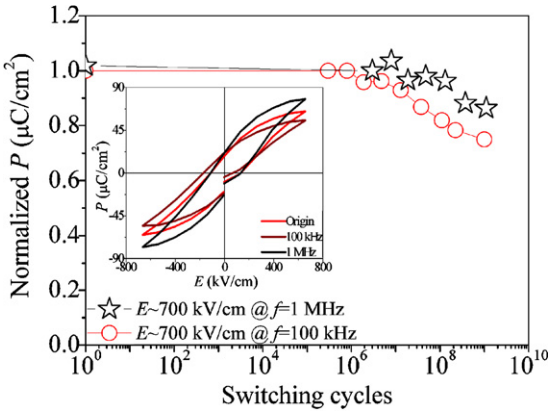

Fig. 7. Fatigue behavior for the BFO/BNBTKNN bilayered thin films, where the inset is *P–E* curves before and after fatigue.

has a slightly decrease (~20%) in the polarization until ~10^9 cycles for the BFO/BNBTKNN bilayered thin film. The measurement frequencies seriously affect the fatigue endurance of the BFO/BNBTKNN bilayered thin film, that is, its fatigue endurance is degraded with a decrease in measurement frequencies from 1 MHz to 100 kHz. For a high measurement frequency of 1 MHz, its fatigue endurance begins to decrease at the switching cycle of ~1.3×10^8. However, for the low measurement frequency of 100 kHz, the fatigue endurance begins to decrease at a lower switching cycle of ~1.3×10^7. The polarization value is decreased by ~15–25% from the initial value upon the switching cycle of ~1.0×10^9 at 1 MHz and 100 kHz. *P–E* curves in the inset of Fig. 7 also confirm the change of the fatigue endurance of the BFO/BNBTKNN bilayered thin film as a function of measurement frequencies. When fatigued at a high frequency, oxygen vacancies and deep traps slowly respond to the driving electric fields for such a bilayer, and the free carriers from top and bottom electrodes mainly make up for the polarization charges [16,24]. Therefore, the slight decrease in polarization value is observed for the bilayer. However, oxygen vacancies transport easily and the trapped charges respond steadily to externally driving electric fields when fatigued at a low frequency [16,24]. The ferroelectric domain switching is blocked by the rearrangement of oxygen vacancies, resulting in a quick decrease in polarization value [25].

4. Conclusion

Multiferroic BFO/BNBTKNN bilayered thin film was fabricated on Pt/TiO_2/SiO_2/Si substrates without any buffer layers by using a combined sol–gel and radio frequency sputtering route. Effect of BNBTKNN on electrical properties of BFO thin film was investigated. The BNBTKNN layer improves the phase purity and the microstructure of the bilayered thin film, resulting in a low leakage current density. Moreover, the BFO/BNBTKNN bilayered thin film has a good dielectric behavior, a good fatigue endurance, and an improved multiferroic behavior of $2P_r$ ~ 76.8 μC/cm^2, $2E_c$ ~ 378.1 kV/cm, $2M_s$ ~ 52.6 emu/cm^3, and $2H_c$ ~ 453.6 Oe.

Acknowledgement

The author gratefully acknowledges the support of Natural Science Foundation for the Youth of the Guizhou University (2009-054).

References

[1] J. Wang, J.B. Neaton, H. Zheng, V. Nagarajan, S.B. Ogale, B. Liu, D. Viehland, V. Vaithyanathan, D.G. Schlom, U.V. Waghmare, N.A. Spaldin, K.M. Rabe, M. Wuttig, R. Ramesh, Science 299 (2003) 1719.
[2] J.F. Li, J.L. Wang, M. Wuttig, R. Ramesh, N. Wang, B. Ruette, A.P. Pyatakov, A.K. Zvezdin, D. Viehland, Appl. Phys. Lett. 84 (2004) 5261.
[3] W. Eerenstein, N.D. Mathur, J.F. Scott, Nature (London) 442 (2006) 759.
[4] R. Ramesh, N.A. Spaldin, Nat. Mater. 6 (2007) 21.
[5] C.W. Nan, M.I. Bichurin, S.X. Dong, D. Viehland, G. Srinivasan, J. Appl. Phys. 103 (2008) 031101.
[6] G. Catalan, J.F. Scott, Adv. Mater. 21 (2009) 2463.
[7] L.W. Martin, Y.H. Chu, R. Ramesh, Mater. Sci. Eng. R 68 (2010) 89.
[8] J. Wu, J. Wang, Acta Mater. 58 (2010) 1688.
[9] X.D. Qi, J. Dho, R. Tomov, M.G. Blamire, J.L. MacManus-Driscoll, Appl. Phys. Lett. 86 (2005) 062903.
[10] J. Wu, J. Wang, J. Appl. Phys. 107 (2010) 034103.
[11] C.C. Lee, J.M. Wu, Appl. Phys. Lett. 91 (2007) 102906.
[12] J. Wu, G. Kang, H. Liu, J. Wang, Appl. Phys. Lett. 94 (2009) 172906.
[13] H.Y. Zhao, H. Kimura, Z.X. Cheng, X.L. Wang, T. Nishida, Appl. Phys. Lett. 95 (2009) 232904.
[14] J.G. Wu, J. Wang, D.Q. Xiao, J.G. Zhu, J. Mater. Chem. 21 (20) (2011) 7308.
[15] D. Xie, Y. Zang, Y. Luo, X. Han, T. Ren, L. Liu, J. Appl. Phys. 105 (2009) 084109.
[16] J.G. Wu, J. Wang, D.Q. Xiao, J.G. Zhu, J. Appl. Phys. 109 (2011) 074101.
[17] J.G. Wu, J. Wang, D.Q. Xiao, J.G. Zhu, Phys. Stat. Sol.-Rapid Res. Lett. 5 (2011) 83.
[18] N.M. Murari, R. Thomas, R.E. Melgarejo, S.P. Pavunny, R.S. Katiyar, J. Appl. Phys. 106 (2009) 014103.
[19] S.K. Singh, H. Ishiwara, K. Sato, K. Maruyama, J. Appl. Phys. 102 (2007) 094109.
[20] Y. Fan, T.J. Zhu, M.O. Lai, L. Lu, Scripta Mater. 63 (2010) 780.
[21] Z.X. Cheng, X.L. Wang, Phys. Rev. B 75 (2007) 172406.
[22] J. Wu, J. Wang, J. Am. Ceram. Soc. 93 (2010) 2795.
[23] S.T. Zhang, A.B. Kounga, E. Aulbach, T. Granzow, W. Jo, H.J. Kleebe, J. Rödel, J. Appl. Phys. 103 (2008) 034107.
[24] L. Pintilie, I. Vrejoiu, D. Hesse, M. Alexe, Appl. Phys. Lett. 88 (2006) 102908.
[25] J.F. Scott, M. Dawber, Appl. Phys. Lett. 76 (2000) 3801.